Evaluation of the Number of Agonist Molecules Needed to Activate a Ligand-Gated Channel from the Current Rising Phase

E. Ratner, O. Tour, and H. Parnas
The Otto Loewi Minerva Center for Cellular and Molecular Neurobiology and the Department of Neurobiology, the Hebrew University, Jerusalem 91904, Israel

ABSTRACT We propose a new method for calculating the number of agonist binding sites (n) in ligand-gated receptor channels from the initial phase of the current. This method is based on the fact that the relation between the current (I) and its first-time derivative (I') at the beginning of the current reflects the number of transitions that lead to channel opening. We show that, for constant agonist concentration, the above relationship at $t \rightarrow 0$ provides the number of steps leading to channel opening. When the agonist concentration is not constant but rather increases linearly with time, the corresponding value can be obtained using a slightly modified procedure. The analytical results were compared with computer simulations and a good match between the two was obtained. The theoretical procedure was then validated experimentally using the nicotinic receptor, because, for this receptor, the number of binding sites is well established. Indeed, the expected number of two binding sites was obtained. The method was then tested for the quisqualate-type glutamate receptor channel from the opener muscle of crayfish. The number of this receptor's binding sites is not fully resolved. Our results suggest that, for this glutamate receptor as well, two binding sites must be occupied to open the channel.

INTRODUCTION

One of the basic parameters characterizing ligand-gated receptor channels is the number of agonist molecules that must be bound to the receptor to transform it into an open channel. A number of theoretical–experimental approaches have been proposed for evaluating this parameter. The most conventional and widespread method is the Hill plot (see Stryer, 1981, p. 68). This method derives the number of binding sites from the maximal slope of a dose–response curve obtained at low agonist concentrations. Using the Hill plot, the number of binding sites for nicotinic acetylcholine receptors (N-AChR) was found to be two (Land et al., 1984; Colquhoun and Sakmann, 1985; Colquhoun and Ogden, 1988). For the quisqualate-type glutamate receptor, (qGluR), also called the α-amino-3-hydroxy-5-methyl-4-isoxazole-propionic acid (AMPA) receptor (Collingridge and Lester, 1989), the Hill coefficient values vary, with findings of 2 (Johans and Sakmann, 1992; Hestrin, 1992; Tour et al., submitted for publication), 3 (Dudel et al., 1990a), and 5 (Dudel et al., 1990b). These variations may be due in part to the low signal-to-noise ratio at low agonist concentrations (the range from which the Hill coefficient is extracted).

Additional approaches for calculating the number of binding sites have been proposed by different investigators. Bates et al., (1990), used the analysis of two-dimensional dwell-time histograms to calculate the number of binding sites for qGluR and found four closed and four open states for this receptor. However, differences in the calculated maximum likelihood values in models assuming two, three, or four binding sites were small. A similar method, based on analysis of three-dimensional dwell-time histograms for discrimination of different models, was proposed by Magleby and Weiss (1990). This method, however, requires a very long simulation time. Clements and Westbrook (1991), calculated the number of binding sites for *N*-methyl-D-aspartate (NMDA) receptors. These researchers also used the maximum likelihood procedure and found that a model with two binding sites for glutamate and two binding sites for glycine best fits the initial phase of the NMDA receptor currents.

All the numerical methods described above demand preliminary information concerning the kinetic scheme and rate constants of the receptor under study. Without such information, convergence toward a final model is unlikely. It seems, therefore, that an additional method is still needed to resolve the fundamental question of how many agonist molecules must be bound for a channel to open. In the present study, we propose an experimental–theoretical procedure to evaluate this number. According to this procedure, analysis of the initial phase of the current provides the number of binding sites. Below, we show that, unlike the Hill plot procedure, our approach yields the best results at high agonist concentrations, which have a much better signal-to-noise ratio. Using this method for qGluR, we found the number of sites that must be bound for the receptor channel to open to be two.

THEORY

The kinetic model

Several models have been proposed to describe the time course of ligand-gated receptor channels (e.g., del Castillo

Received for publication 17 August 1999 and in final form 17 November 1999.

Address reprint requests to Eli Ratner, Institute of Life Sciences, Department of Neurobiology, The Hebrew University, Jerusalem 91904, Israel. Tel.: +972-2-6585591; Fax: +972-2-6521921; Email: eli@nerve.ls.huji.ac.il.

0006-3495/00/02/731/15 $2.00

and Katz, 1957; Land et al., 1984; McManus et al., 1988; Parnas et al., 1989; Dudel et al., 1990b; Franke et al., 1991; Buchman and Parnas, 1992, 1994; Maconochie et al., 1994; Colquhoun and Hawkes, 1995). Common to all these models is the presumption that the process of channel opening occurs in sequential steps. Accordingly, the receptor first binds the agonist molecules, usually one-by-one in sequence. Then, when the required number of agonist molecules are bound, the receptor undergoes a conformational change resulting in channel opening.

The following is a generalized representation of such a sequential kinetic scheme:

$$R_o + A \underset{k_{-1}}{\overset{k_1}{\longleftrightarrow}} R_1 + A \underset{k_{-2}}{\overset{k_2}{\longleftrightarrow}} \cdots \underset{k_{-1}}{\overset{k_i}{\longleftrightarrow}} R_i + A \underset{k_{-i+1}}{\overset{k_{i+1}}{\longleftrightarrow}} \cdots \underset{k_{-n}}{\overset{k_n}{\longleftrightarrow}} R_n \quad R_n \underset{k_o}{\overset{k_c}{\updownarrow}} O$$

SCHEME 1

R_i denotes a receptor bound to i agonist molecules (i is an integer ranging from 0 to n, where n is the number of sites that must be bound for the channel to open). A stands for the agonist, and O for an open channel. k_i and k_{-i} are forward and backward rate constants, respectively, and k_o and k_c are the channel opening and closing rate constants, respectively. Such schemes have gained appreciable experimental support and are widely accepted.

Variations on Scheme 1 have also been suggested (e.g., Colquhoun and Sakmann, 1985; Bates et al., 1990). However, in many of these variant models, the backbone of Scheme 1 is preserved, with one or more bifurcating branches added. These added branches result in additional openings. Usually, the rate constants associated with these branches are smaller than those associated with the main backbone (Bates et al., 1990; Colquhoun and Hawkes, 1995). Nevertheless, we will consider the validity of our proposed procedure also for the case of more than one open state.

Mathematical model to evaluate the number of binding sites, *n*

The theoretical–experimental procedure proposed here evaluates the number of binding sites from the rising phase of the current. To highlight the essence of the procedure, we first examine the simplest case—constant agonist concentration. By constant agonist concentration, we mean a situation in which, at $t = 0$, agonist concentration is instantly stepped from zero to its assigned level and is kept constant at this level. Such conditions can be reproduced in experiments using outside-out patches with fast application of the agonist (see Fig. 4, *B*, *D*, *F*).

The situation may be different under physiological conditions. Results reported by Clements (1996) and Dudel et al. (1999) suggest that, during the rising phase of the miniature endplate postsynaptic current (MEPSC), the transmitter concentration rises almost linearly with time before it eventually declines. Therefore, we will also expand the proposed theoretical–experimental procedure to include a case in which the agonist concentration is not constant but rather rises linearly with time.

We begin with some intuitive considerations. The number of binding sites in Scheme 1 is n, and the total number of steps leading to channel opening is $n + 1$. Consequently, at $t \to 0$, the open probability P_o is proportional to t^{n+1}, or, in a semi-formal way,

$$\lim_{t\to 0} (P_o) \propto t^{n+1}. \tag{1}$$

The first derivative of P_o, P'_o under the conditions of Eq. 1, is

$$\lim_{t\to 0} (P'_o) \propto (n + 1) \cdot t^n. \tag{2}$$

Dividing Eq. 1 by Eq. 2 gives,

$$\lim_{t\to 0} \left(\frac{P_o}{P'_o}\right) \propto \frac{t}{n + 1}. \tag{3}$$

Deriving Eq. 3, with respect to t, at $t = 0$, we obtain

$$\left(\frac{P_o}{P'_o}\right)'_{t=0} \propto \frac{1}{n + 1}. \tag{4}$$

Equations 2–4 demonstrate the procedure for extracting $n + 1$. Specifically, from the derivative of the ratio (P_o/P'_o) at $t = 0$, we can extract $n + 1$.

Using the Taylor expansion of the function $(P_o/P'_o)(t)$, we proved (see Appendix A, Constant agonist concentration) that, for constant agonist concentration, the proportionality in Eq. 4 can be replaced by equality,

$$\left(\frac{P_o}{P'_o}\right)'_{t=0} = \frac{1}{n + 1}. \tag{5}$$

For linearly increasing agonist concentration, Eq. 5 should be modified (see Appendix A, Linearly increasing agonist concentration) as follows:

$$\left(\frac{P_o}{P'_o}\right)'_{t=0} = \frac{1}{2n + 1}. \tag{6}$$

MATERIALS AND METHODS

Theoretical methods

Implementation of Eqs. 5 and 6

Direct experimental implementation of Eqs. 5 and 6 is impossible for two reasons. First, solution of these equations demands an exact definition of the beginning of the current, a point that is difficult to resolve from

experimental data. Second, the value of $(P_o/P'_o)'$ at $t = 0$, which is necessary to evaluate n, cannot be measured using only one experimental point at $t = 0$. These two difficulties can be circumvented if the rationales underlying Eqs. 5 and 6 are retained while the exact procedure of solution is varied somewhat.

Concerning the first difficulty, we notice that, if the reciprocal function, $t(P_o/P'_o)$ (existence and properties of the reciprocal function are shown in Appendix B), is used instead of $(P_o/P'_o)(t)$ (Eqs. 5 and 6) the need to pinpoint $t = 0$ is replaced by a need to pinpoint $P_o = 0$. This is easier to achieve. The second problem can be circumvented as follows. If we expand the range of measurements from exactly $t = 0$ to a finite range of t in the vicinity of $t = 0$, we can approximate the reciprocal function $t(P_o/P'_o)$ by a polynomial function. The first derivative of this polynomial function can be used instead of the derivative of $t(P_o/P'_o)$ for calculation of $n + 1$ (Eq. 5) or $2n + 1$ (Eq. 6).

The polynomial function is obtained by a Taylor expansion of $t(P_o/P'_o)$ (Courant, 1937b),

$$t\left(\frac{P_o}{P'_o}\right) = t_0 + \sum_{j=1}^{\infty} b_j \cdot \left(\frac{P_o}{P'_o}\right)^j. \tag{7}$$

Here, b_j stands for a constant coefficient of a jth polynomial term (j is an integer ranging from 1 to ∞).

To extract n from the polynomial function (Eq. 7), we repeat the procedure used for the direct function. We thus derive Eq. 7 at $P_o/P'_o = 0$,

$$\left(t\left(\frac{P_o}{P'_o}\right)\right)'_{(P_o/P'_o)=0} = b_1. \tag{8}$$

Here, b_1 is the first polynomial coefficient. Also, according to the theorem of the reciprocal function (Courant, 1937a), the left side of Eq. 8 equals

$$\left(t\left(\frac{P_o}{P'_o}\right)\right)'_{(P_o/P'_o)=0} = \frac{1}{(P_o/P'_o)'_{t=0}}. \tag{9}$$

Combining Eqs. 8 and 9, we obtain

$$b_1 = \frac{1}{(P_o/P'_o)'_{t=0}}. \tag{10}$$

Incorporating Eq. 5, for constant agonist concentration, into Eq. 10 we obtain

$$b_1 = \frac{1}{[1/(n+1)]} = n + 1. \tag{11}$$

Incorporating Eq. 6, for linearly increasing agonist concentration, into Eq. 10 we obtain

$$b_1 = \frac{1}{[1/(2n+1)]} = 2n + 1. \tag{12}$$

Actual evaluation of b_1

Fitting the infinite-order polynomial (Eq. 7) to the actual experimental data is impossible. Therefore, we must truncate Eq. 7 to finite-order polynomials. For later use, we notice that the first-order polynomial is given by

$$t\left(\frac{P_o}{P'_o}\right) = t_0 + b_1 \cdot \left(\frac{P_o}{P'_o}\right), \tag{13}$$

the second-order polynomial is given by

$$t\left(\frac{P_o}{P'_o}\right) = t_0 + b_1 \cdot \left(\frac{P_o}{P'_o}\right) + b_2 \cdot \left(\frac{P_o}{P'_o}\right)^2, \tag{14}$$

and the third-order polynomial is given by

$$t\left(\frac{P_o}{P'_o}\right) = t_0 + b_1 \cdot \left(\frac{P_o}{P'_o}\right) + b_2 \cdot \left(\frac{P_o}{P'_o}\right)^2 + b_3 \cdot \left(\frac{P_o}{P'_o}\right)^3. \tag{15}$$

Assessment of b_1 from the finite-order polynomials (Eqs. 13–15) will yield a smaller value than expected, based on the infinite-order polynomial (Eqs. 11 and 12). Hence, we must seek the maximal value of P_o (denoted as P_v) that still guarantees a valid value of b_1; i.e., will satisfy the condition of

$$n + 1 \geq b_1 \geq n \tag{16}$$

for constant agonist concentration, and the condition of

$$2n + 1 \geq b_1 \geq 2n - 1 \tag{17}$$

for linearly increasing agonist concentration.

Even though we are interested in b_1 only, b_2 (Eq. 14 and 15) and b_3 (Eq. 15) must satisfy certain conditions for the evaluation of b_1 to be correct. In Appendix C, we show that, for both constant and linearly increasing agonist concentrations, these conditions are

$$b_2 < 0 \qquad b_3 > 0. \tag{18}$$

The theoretical approach presented above is general for any number (n) of binding sites and does not depend on the value of the rate constants involved. Neither does it depend on experimental conditions such as temperature or agonist concentration (excluding the requirement of constant agonist concentration). By contrast, P_v can be strongly affected by all the above parameters. Therefore, P_v must be evaluated under various conditions, such as agonist concentration and temperature.

Because we cannot find the value of P_v analytically, we turn to computer simulations. The appropriate P_v depends, as mentioned above, on n itself. This leads to the question of the n to be used in simulations. In determining the value of n for the simulation, we take the following factors into consideration. If P_v is selected to determine n, say, of two, and the actual n of the receptor under study is higher than two, we will not be able to extract this higher n. However, if P_v is selected to yield a high n, it will still be absolutely suitable for yielding a lower n. Therefore, at least for the nicotinic receptor, a good practice is to assign a value of 3 to n in the simulations to determine the appropriate P_v. For an unknown receptor, it is also advisable to select P_v suitable for $n = 3$ and change this only if the analysis suggests a higher n.

Three agonist concentrations were considered: low (0.01 mM), medium (0.1 mM), and high (1 mM). The values of the rate constants were taken to be those corresponding to the AChR in the frog neuromuscular junction. For the high temperature, we took the parameters' values to be those provided by Franke et al. (1991) (Table 1) and modified them slightly for a model containing three binding sites. The effect of the temperature was modeled by lowering the values of all rate constants.

Because the influence of the experimental noise on the approximated polynomial increases with the order of the polynomial, we decided to obtain P_v only for the first-, second-, and third-order polynomials. We begin with the first-order approximation (linear approximation) for constant agonist concentration (Eq. 13). The procedure for finding P_v in this case is exemplified in Fig. 1, *A* and *B*. We simulated the model with $n = 3$, and transformed the obtained function $P_o(t)$ (shown on Fig. 1 *A*) into the function $t(P_o/P'_o)$ (Fig. 1 *B*, *empty squares*). Next, the linear function was fitted to function $t(P_o/P'_o)$ on a wide range of P_o (*dashed line*). Then the range of P_o was sequentially decreased until the slope of the linear fit, b_1, reached the correct value of $b_1 > 3$ (*solid line*, see Eq. 16). The maximal value of P_v, required by the first-order polynomial, was obtained at high

TABLE 1 Values of rate constants for Scheme 1

Rate Constant	Fast Kinetic Model, $n = 3$	Slow Kinetic Model, $n = 3$	Slow Kinetic Model, $n = 2$
k_1	300	60	40
k_2	200	40	20
k_3	100	20	–
k_{-1}	10	2	4
k_{-2}	20	4	8
k_{-3}	30	6	–
k_o	50	10	10
k_c	1.1	0.22	0.22

For the fast kinetic model (room temperature), we modified the rate constants taken from Franke et al., 1991, for the model with $n = 3$. The slow kinetic model (low temperature) was achieved by lowering all rate constants fivefold. Units: k_1, k_2, k_3 = $mM^{-1}ms^{-1}$, k_{-1}, k_{-2}, k_{-3}, k_o, and k_c = ms^{-1}.

agonist concentration and low temperature. This very small current of $P_v = 0.004 \cdot P_{max}$ cannot be measured accurately. Therefore, we must increase the order of the polynomial and use Eqs. 14 and 15 instead of Eq. 12. Eqs. 14 and 15 allow us to increase the range of P_v.

Fig. 1 *C* shows an example using Eqs. 14 and 15. Second- (*striped line*) and third- (*solid line*) order polynomials were fitted to the simulation results (*open squares*). For the second-order polynomial, $P_v = 0.08 \cdot P_{max}$. For the third-order polynomial, $P_v = 0.25 \cdot P_{max}$.

The same procedure was performed for the linearly increasing agonist concentration (Fig. 2, *A* and *B*). With the exception of agonist concentration, which rose from 0 to 1 mM over 0.3 ms, the parameters for the simulations were the same as those used for Fig. 1, *A*, *B*, and *C*. For the second-order polynomial (Fig. 2 *B*, *striped line*), $P_v = 0.16 \cdot P_{max}$. For the third-order polynomial (Fig. 2 *B*, *solid line*), $P_v = 0.39 \cdot P_{max}$. These values are even larger than those obtained for constant agonist concentration, rendering the estimation of n easier.

Computer simulations and data analysis

Differential equations were solved using the fourth-order Runge–Cutta method. Stochastic behavior of the channels was modeled as a series of single-channel simulations that used the Monte-Carlo method. All simulations were performed on SGI (Indy, Unix Irix 5.3, SGI Inc., Mountain View, CA) workstations using BIOQ, a program developed in our laboratory (Ashkenazi and Parnas, 1997). Data analyses were performed on a PC using Microsoft Excel.

Experimental methods

Preparations and experimental conditions

Frog. Miniature endplate postsynaptic currents (MEPSCs) were recorded from the cutaneous pectoris neuromuscular junction (NMJ) of a frog (*Rana ridibunda*). The preparation was isolated using the technique elaborated by Bloch et al. (1968) and was bathed in a standard solution (Dudel, 1989). Temperature was kept at 8 ± 1°C.

Crayfish. MEPSCs were recorded from the opener neuromuscular system of a crayfish, *Procambus clarkii* (Dudel and Kuffler, 1961), and single-channel currents were recorded from the crayfish deep abdominal extensor muscles (Parnas and Atwood, 1966). The preparations were bathed in standard van Harreveld solutions (Franke et al., 1987), at a temperature of 12 ± 1°C. Patch electrodes for outside-out recordings were filled with intracellular low Cl^- solution (Franke et al., 1987).

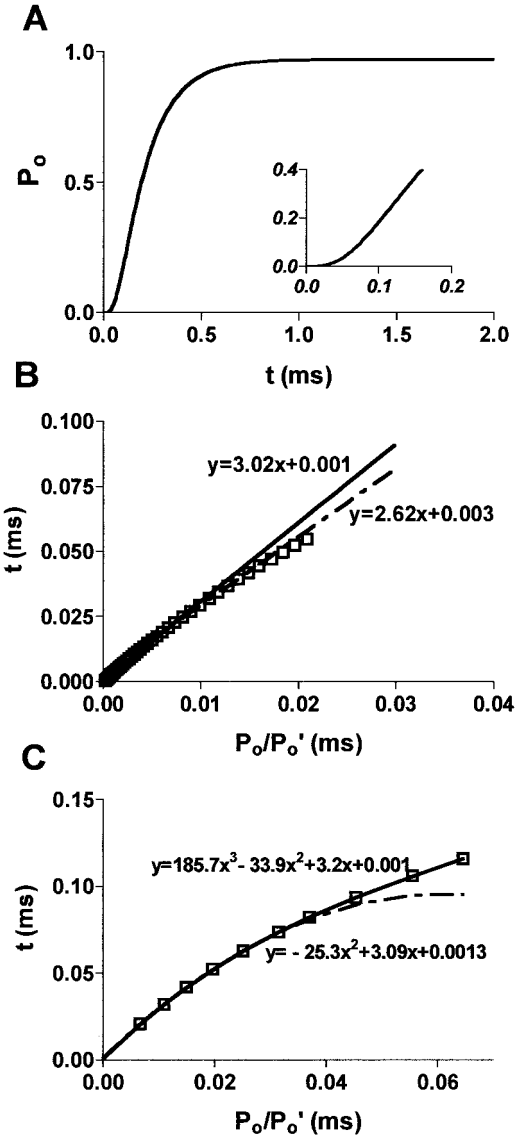

FIGURE 1 Results of simulations of a three-binding-sites model ($n = 3$) used for extracting P_v at constant agonist concentration. A standard slow set of parameters was used for simulations (Table 1). (*A*) Time course (*solid line*) of the open probability at 1 mM of agonist. The magnified initial phase is shown in the insert. (*B*) Results of the first-order approximation of the function $t(P_o/P_o')$ (Eq. 13). *Empty squares*, values of the function; *striped line*, linear fit at $t = 0.03$ ms ($b_1 = 2.62$, suggesting two binding sites instead of three, see Eq. 17); *solid line*, linear fit at $t = 0.025$ ms ($b_1 = 3.02$, suggesting the correct number, 3, of binding sites). In this case, $P_v = 0.004 \cdot P_{max}$. (*C*) Second- (Eq. 14, *striped line*) and third- (Eq. 15, *solid line*) order polynomial approximation of $t(P_o/P_o')$ (*empty squares*). For the second-order polynomial approximation, P_v was found to be $0.08 \cdot P_{max}$ ($b_1 = 3.09$). For the third-order polynomial approximation, P_v was found to be $0.25 \cdot P_{max}$ ($b_1 = 3.2$).

MEPSC recordings and averaging

For both the frog and the crayfish, the standard macropatch technique (Dudel, 1983) was used to stimulate the preparation and record the currents. Each preparation was stimulated 5–10 thousand times at 2–3 Hz. Quantal content was in the range of 0.2. MEPSCs from each experiment

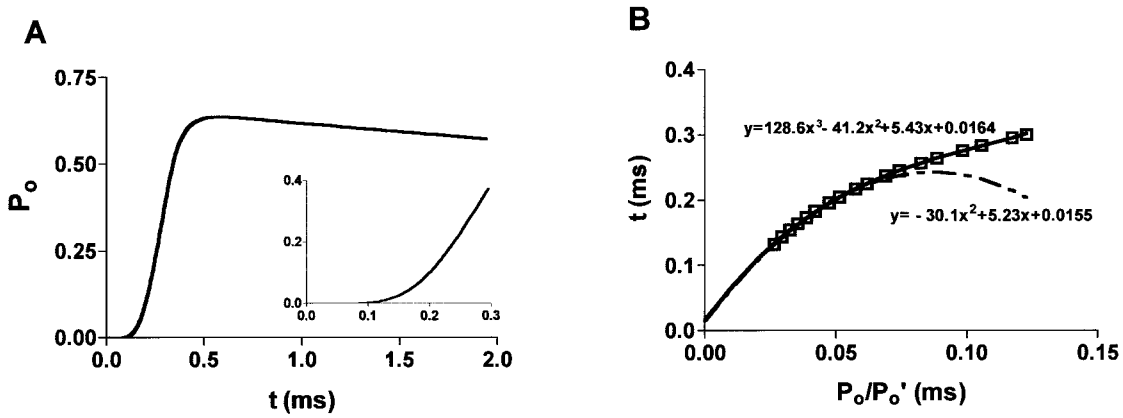

FIGURE 2 Results of simulations of a three-binding-sites model ($n = 3$) used for extracting P_v with linearly increased agonist concentration. A standard slow set of parameters was used for simulations (Table 1). (*A*) The time course (*solid line*) of the open probability. Agonist concentration was increased linearly from 0 to 1 mM for 0.3 ms and then decreased exponentially. The insert shows the magnified initial phase. (*B*) Second- (Eq. 14, *striped line*) and third- (Eq. 15, *solid line*) order polynomial approximation of $t(P_o/P_o')$ (*empty squares*). For the second-order polynomial approximation, P_v was found to be $0.16 \cdot P_{max}$ ($b_1 = 5.23$, $n = 3$, see Eq. 17). For the third-order polynomial approximation, $P_v = 0.39 \cdot P_{max}$ ($b_1 = 5.43$, $n = 3$).

were recorded separately at a sampling rate of 100 kHz, using the LabView interface (AT-MIO-16F-5, NI-DAQ 4.9.0 driver software, National Instrument Corporation, Austin, TX). A preliminary selection of traces was made by excluding all traces with zero or multiple MEPSCs. The remaining MEPSCs were then aligned (using our own programs developed for this purpose) as follows: To measure the baseline (Fig. 3 *A*, *striped line*) and the peak value (marked as 1), we subjected the raw data (*solid line*) to a 10-kHz filter (*dashed line*). The rise time (t_r, 10–90% of peak current) was then measured and averaged. All traces in which t_r differed from the average t_r by more than 10% were excluded. Because it is impossible to pinpoint the exact beginning of the current, we defined an effective beginning as 10% of the peak value (marked as 2). All traces were aligned to this point. Traces in which the noise level in the vicinity of this point exceeded 10% of the peak current were excluded from further processing.

Following the steps described, 50–200 traces remained suitable for averaging. These aligned nonfiltered traces were averaged (Fig. 3, *B* and *C*).

Single channel recording and averaging

The fast application system used for applying pulses of glutamate (L-glutamic acid sodium salt, BDH, Poole, UK) to the outside-out patches has been described in detail (Franke et al., 1987; Dudel et al., 1990b). Briefly, a well-defined thin liquid filament was produced by using pressure to eject a solution containing the agonist from a polyethylene tube glued to a steel needle. The tube was moved rapidly by a piezo crystal so that the liquid filament washed the tip of a patch pipette. The speed of solution exchange at the pipette tip depends primarily on the velocity of the ejected solution (Maconochie and Knight, 1989). Speed of solution exchange at the tip of an open patch pipette was tested as follows (Maconochie et al., 1989). The solution was diluted in the liquid filament by 20% to produce a junction potential so that currents (osmotic currents) could be recorded when switching from the control solution to a diluted one. In some experiments, fast application of the agonist was needed, although, in others, slow application was required. The ejected solution velocities used for such applications were 300 and 100 mm/msec, respectively. The shapes of the osmotic current profiles for both cases were recorded with an open pipette. The 10–90% rise time for the slow application was 310 μs (Fig. 4 *A*). For the fast application, it was 160 μs (Fig. 4 *B*).

An example of one recorded trace of channel activity in response to a slow application of 10 mM glutamate is shown in Fig. 4 *C* (*thin solid line*). The heavy solid line is the outcome of averaging 1000 such traces. Electrical artifacts and leak currents were eliminated from the glutamate-activated ensemble currents by subtracting average currents recorded from the same patch where glutamate was absent from the applied solution (Fig. 4 *C*, *striped line*). The magnified initial phase of the resulting current is shown in Fig. 4 *E*. Each patch was then analyzed separately. Currents activated by fast glutamate application were analyzed and averaged in the same manner (Fig. 4, *D* and *F*).

Averaged data is given as the mean ± SD.

RESULTS

The total current through the channels is proportional to the open probability. We can therefore use the function $t(I/I')$ instead of $t(P_o/P_o')$ in Eqs. 14 and 15.

Evaluation of *n* for the nicotinic receptor from MEPSCs

Because an n of two is well established for N-AChR (Rang, 1974; Prinz and Maelicke, 1983; Unwin, 1993; Hucho et al., 1996; see also references in Introduction), we began our study with this receptor to test the validity of our theory. The MEPSCs were recorded, aligned, and averaged as described in Materials and Methods (Fig. 3, *A* and *B*). Then, the rising phases of the aligned and averaged currents were analyzed as described in Eqs. 14 and 15. Analysis for one experiment is shown in Fig. 5 *A*. A second-order polynomial (Eq. 14, *dashed line*) was successfully fitted to the experimental data points (*empty squares*) of $t(I/I')$ at the range of $0.025 \cdot I_{peak}$–$0.22 \cdot I_{peak}$. The first derivative of this polynomial, b_1 (Eqs. 12 and 16 are used, as the ACh concentration in the synaptic cleft increases linearly with time), at $(I/I') = 0$, is 4.41, implying $n = 2$ (Eq. 17). The third-order polynomial (*solid line*) was fitted to the range of $0.025 \cdot I_{peak}$–$0.37 \cdot I_{peak}$, with $b_1 = 3.92$, also implying $n = 2$. This experiment was repeated 14 times. Second-

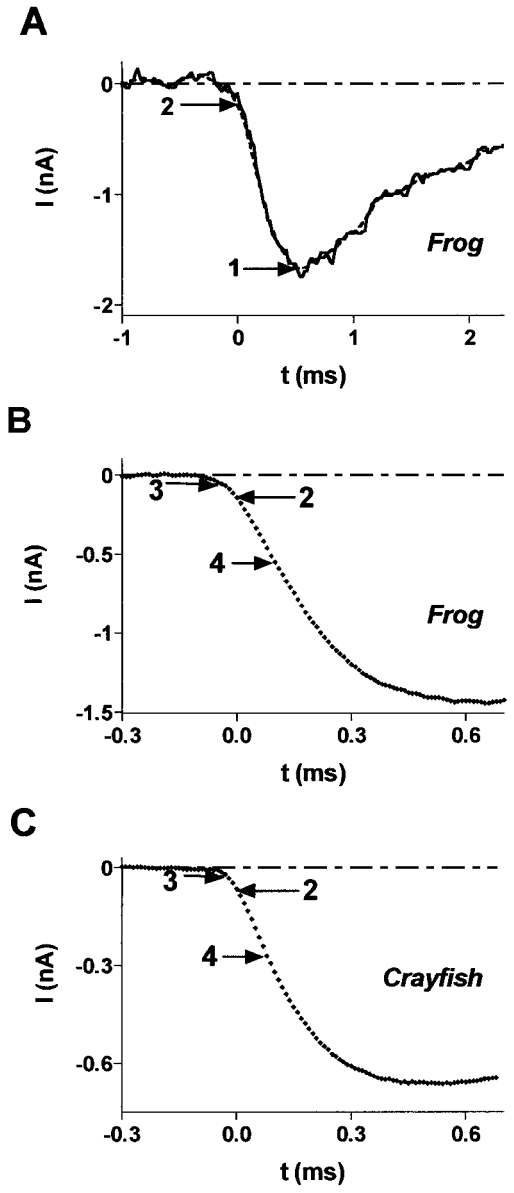

FIGURE 3 MEPSCs: recordings and averaging. (*A*) Single MEPSC recorded from frog neuromuscular junction (N-AChR receptor). *Solid line*, one example of raw data; *dashed line*, the same MEPSC filtered at 10 kHz. Baseline (*striped line*) was calculated by averaging 50 points before the rising phase of the current. The peak value of the current (1) is calculated from the filtered current. The point of alignment (2) is chosen as the point at which the value of the nonfiltered current is equal to 0.1 of the peak value. Here, and in all the following figures showing experimental results, time zero (abscissa) was chosen to be this alignment point. (*B*) Rising phase (points) of an average current of 98 synchronized MEPSCs recorded from frog neuromuscular junction. The baseline and the synchronization point (2) were determined as in *A*. The current in the range between points 3 and 4 is used for analyzing the number of agonist binding sites. (*C*) The same as *B*, recorded from crayfish neuromuscular junction (qGluR receptor).

order polynomials were successfully fitted for 12 of 14 experiments. In 2 of 12 cases, b_1 was smaller than 3 (suggesting one binding site); in 10 of 12 cases, b_1 was greater than 3 and smaller than 5 (suggesting two binding sites). The second-order polynomials fitted to the remaining two patches did not meet the requirements set in Eq. 18. The average value of b_1 for the second-order polynomials was 3.75 ± 0.62. Third-order polynomials were successfully fitted to 11 of 14 cases. In 2 of 11 cases, b_1 was smaller than 3 (suggesting one binding site); in 9 of 11 cases b_1 was greater than 3 and smaller than 5 (suggesting two binding sites). For the remaining 3 patches, a third-order polynomial did not meet the requirements set in Eq. 18. The average value of b_1 for the third-order polynomials was 3.74 ± 0.62. These results are summarized in Table 2.

Evaluation of *n* for the quisqualate receptor from MEPSCs

The procedure described above was repeated for the glutamate receptor, qGluR. Analysis for one experiment is shown in Fig. 5 *B*. The function $t(I/I')$ was approximated by second- (*dashed line*) and third- (*solid line*) order polynomials. The second-order polynomial was fitted to the range from $0.02 \cdot I_{peak}$ to $0.18 \cdot I_{peak}$, and the third-order polynomial was fitted to the range from $0.02 \cdot I_{peak}$ to $0.34 \cdot I_{peak}$. The values of b_1 were 3.56 in both cases, suggesting $n = 2$ (Eq. 17). The experiment was repeated 21 times. The average values of b_1 were 3.75 ± 0.43 for the second-order polynomial and 3.84 ± 0.51 for third-order polynomial. The results are summarized in Table 2.

Evaluation of *n* for the quisqualate receptor from outside-out recordings (slow application of glutamate)

A solution of 10 mM glutamate was slowly applied (see Materials and Methods) 1000 times to a patch, containing qGluRs. The recorded currents were averaged as described in Materials and Methods. In this case as well, n was evaluated from Eqs. 12 and 17, because the slow application of agonist causes the agonist concentration to rise almost linearly with time (see Fig. 4 *A*). The results of one experiment are shown in Fig. 5 *C*. The data points (*empty squares*) of $t(I/I')$ were approximated by second- (*dashed line*) and third- (*solid line*) order polynomials. The fit range for the second-order polynomial was from $0.02 \cdot I_{peak}$ to $0.23 \cdot I_{peak}$. For the third-order polynomial, it was from $0.02 \cdot I_{peak}$ to $0.38 \cdot I_{peak}$, with a b_1 of 3.45 and 3.18, respectively, both suggesting $n = 2$ (Eq. 17). Eleven such experiments were conducted, and the results are summarized in Table 2.

Evaluation of *n* for the quisqualate receptor from outside-out recordings (fast application of glutamate)

In this type of experiment, we tried to create the conditions that would satisfy Eqs. 11 and 16. To do so, a fast applica-

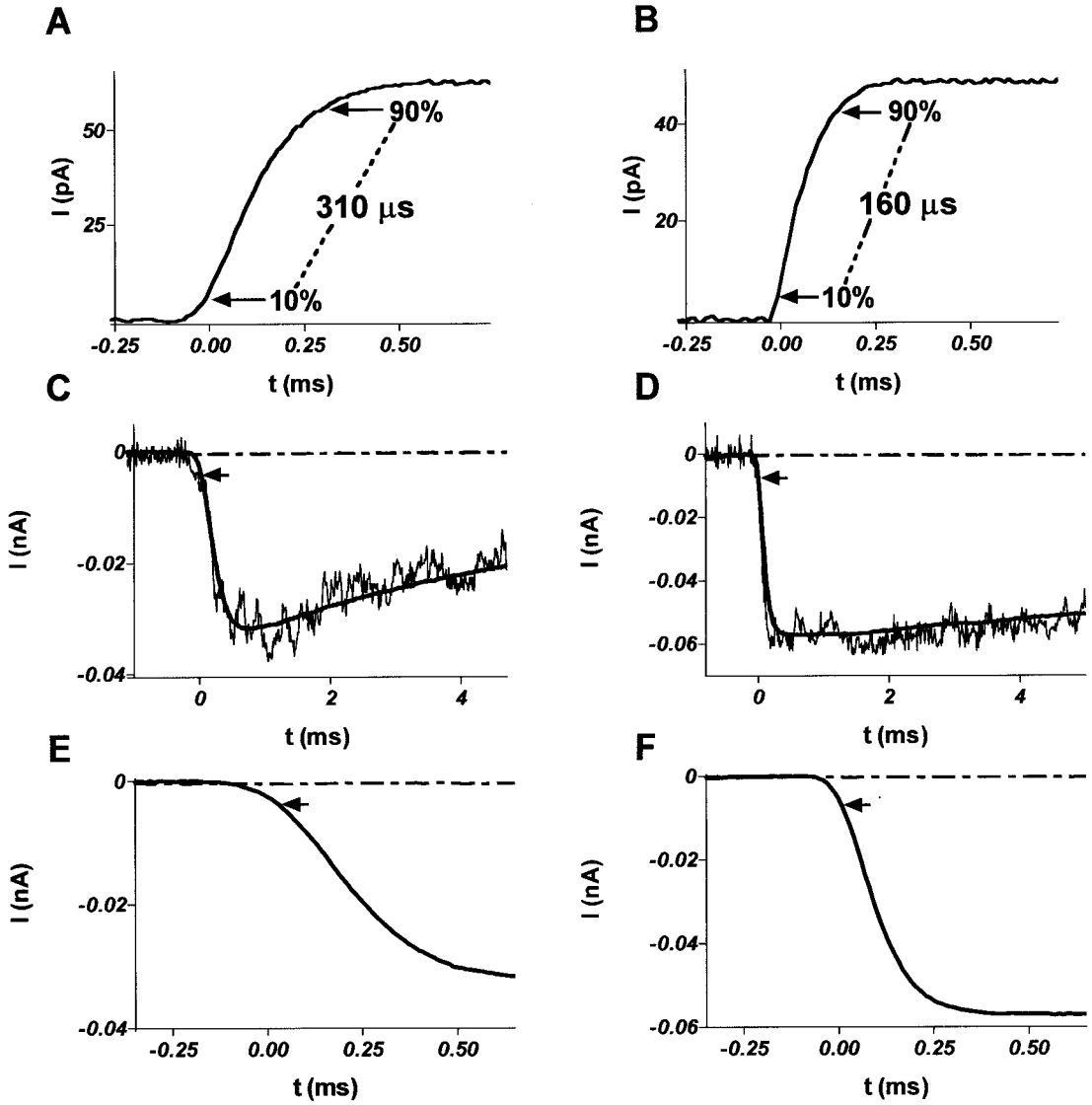

FIGURE 4 Outside-out patch recordings from glutamate channels activated by slow (*A*, *C*, *E*) and fast (*B*, *D*, *F*) application of glutamate. (*A*) The time course of the solution exchange at an open patch pipette was tested using osmotic currents. The velocity of the ejected solution was ~100 μm/msec (slow application). The exchange of the solution, expressed as the rise time of the current (10–90%) took 310 μsec. (*B*) Same as *A* but for a case where the velocity of the ejected solution was ~300 μm/msec (fast application). Here, the exchange in solutions (10–90%) took 160 μsec. (*C*) One example (*thin solid line*) of current elicited by slow application of 10 mM glutamate to an outside-out patch with a holding potential of −70 mV. The outcome of averaging 1000 such currents is the heavy solid line. The base line (*striped line*) was established by averaging 1000 applications of glutamate-free solution on the same patch. (*D*) Same as *C* but for the fast application of glutamate. (*E*) and (*F*) are the rising phases of the averaged currents depicted in *C* and *D*, respectively, shown in more detail.

tion procedure was used (see Materials and Methods and Fig. 4 *B*). The results of one experiment are shown in Fig. 5 *D*. A second-order polynomial was fitted to the function $t(I/I')$ at a range of $0.02 \cdot I_{peak}$ to $0.2 \cdot I_{peak}$. We selected a wider range than required by Eq. 14 to decrease the influence of the noise near the point $(I/I') = 0$. As will be discussed, the widening of the fitting range is partially compensated by the noninstantaneous application of glutamate. The value of b_1 is 2.94, reconfirming two binding sites ($n = 2$) for qGluR (Eq. 16). We did not repeat the analysis with a third-order polynomial (Eq. 15), because, in this case, the requirements set by Eq. 18 could not be met. This experiment was repeated 16 times. In all 16 cases, a second-order polynomial was successfully fitted, although a third-order polynomial could fit only 2 out of 16 experiments. The results are summarized in Table 2.

The robustness of the proposed method

To check for the robustness of the proposed theoretical–experimental method, we turn to an examination of factors that may affect the precision of the evaluation of *n*.

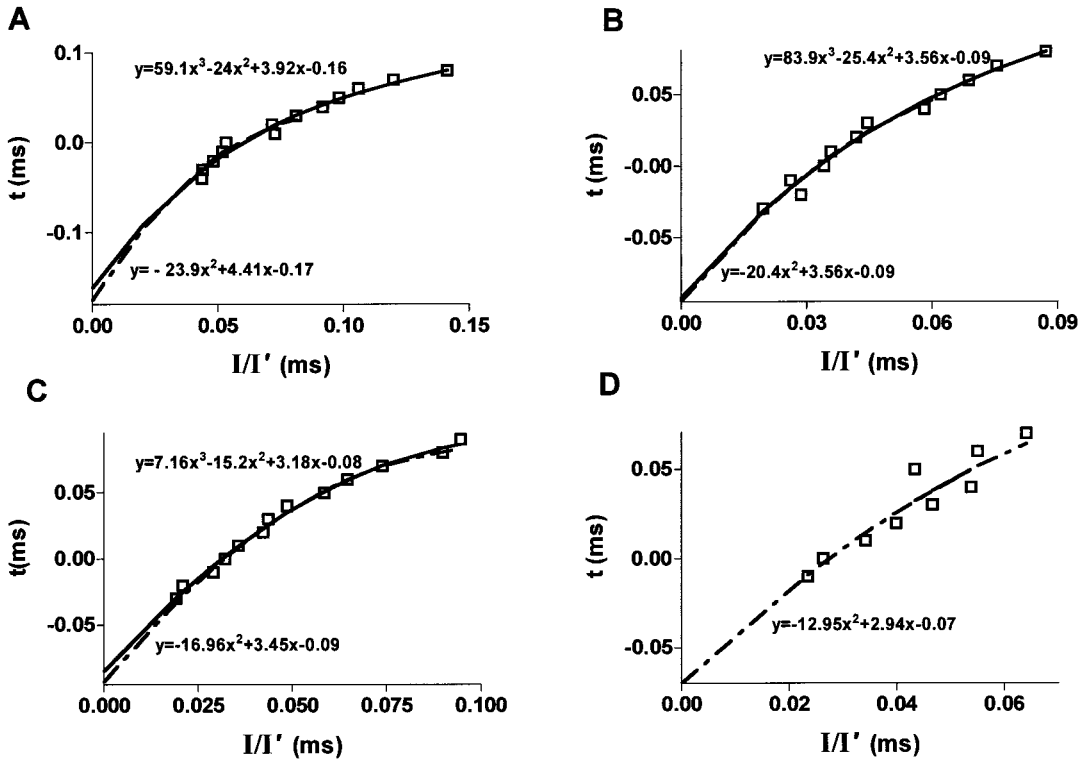

FIGURE 5 Examples of the polynomial fits of the function $t(I/I')$ calculated for the different types of experiments. *Empty squares*, calculated values of $t(I/I')$; *striped line*, second-order polynomial approximation (Eq. 14); and *solid line*, third-order polynomial approximation (Eq. 15). The value of n is calculated using Eq. 17 for (*A*), (*B*), and (*C*), and using Eq. 16 for (*D*). (*A*) The analysis of averaged MEPSC recorded from N-AChR (Fig. 3 *B*). The fitting range for the second-order polynomial is from $0.025 \cdot I_{peak}$ to $0.22 \cdot I_{peak}$. The obtained value of $b_1 = 4.41$; therefore $n = 2$. The fitting range for the third-order polynomial is from $0.025 \cdot I_{peak}$ to $0.37 \cdot I_{peak}$. The obtained value of $b_1 = 3.92$, therefore $n = 2$. (*B*) Analysis of averaged MEPSC (qGluR, Fig. 3 *C*). The fitting range for the second-order polynomial is from $0.02 \cdot I_{peak}$ to $0.18 \cdot I_{peak}$. The obtained value of $b_1 = 3.56$; therefore $n = 2$. The fitting range for the third-order polynomial is from $0.02 \cdot I_{peak}$ to $0.34 \cdot I_{peak}$. The obtained value of $b_1 = 3.56$; therefore $n = 2$. (*C*) Analysis of the averaged currents recorded using the patch clamp technique with slow agonist application (Fig. 4, *A*, *C* and *E*) recorded for qGluR. The fitting range for the second-order polynomial is from $0.02 \cdot I_{peak}$ to $0.2 \cdot I_{peak}$. The obtained value of $b_1 = 3.45$; therefore $n = 2$. The fitting range for the third-order polynomial is from $0.02 \cdot I_{peak}$ to $0.38 \cdot I_{peak}$. The obtained value of $b_1 = 3.18$; therefore $n = 2$. (*D*) Analysis of the averaged currents recorded using the Patch clamp technique with fast application of the agonist. A second-order polynomial was fitted to the range from $0.02 \cdot I_{peak}$ to $0.2 \cdot I_{peak}$. The obtained value of $b_1 = 2.94$; therefore, $n = 2$. A third-order polynomial was not fitted in this case, because it does not meet the condition of Eq. 18.

Stochastic noise

The real experimental data includes stochastic noise that results from the stochastic behavior of the channels. To check the effect of the stochastic noise on our results, we replaced the deterministic model used previously (Figs. 1 and 2) with a Monte-Carlo model. Figure 6, *A* and *B* shows the results of one simulation with $n = 3$ and linearly increasing agonist concentration. The resulting current (Fig. 6 *A*, *filled diamonds*) is an average of 10,000 single-channel currents (representing the average of 100 MEPSCs when each one consists of 100 single-channel currents). Transformation of this current in Fig. 6 *A* (in range marked by the dashed lines) to the function $t(P_o/P'_o)$ is shown in Fig. 6 *B* (*empty squares*). As shown, a third-order polynomial (Eq. 15, *solid line*) was successfully fitted to these data points. The value of $b_1 = 5.86$ was obtained. Eleven such simulations were performed. A third-order polynomial was successfully fitted to nine of them (the other two simulations did not meet the requirements set in Eq. 18) with the following results: b_1 values were $5 < b_1 < 7$ (suggesting three binding sites) in five simulations, $7 < b_1 < 9$ (suggesting four binding sites) in one simulation, and $3 < b_1 < 5$ (suggesting two binding sites) in three simulations. The average value of $b_1 = 5.39 \pm 1.31$, suggests the correct number, of $n = 3$.

More than one open state

Colquhoun and Sakmann (1985) reported that N-AChR exhibits two open states: one from a single-liganded receptor and the main open state from a double-liganded receptor. For this receptor, we found that $n = 2$ (Fig. 5 *A*). How strong, then, must the opening from the singly bound receptor be for the observed n to be one and not two? To answer this question, we conducted a simulation with the

TABLE 2 Experimental results

Experiment	Number of Experiments (N)			Average Fit Range (fraction of I_{max})		b_1 Range		b_1 Average		N, Suggested 1, 2, and 3 Binding Sites					
	Total	2nd	3rd	2nd	3rd	2nd	3rd	2nd	3rd	2nd			3rd		
										1	2	3	1	2	3
1. Synaptic currents, AChR	14	12	11	0.026–0.20	0.025–0.33	2.67–4.65	2.72–4.94	3.75 ± 0.62	3.74 ± 0.62	2	10	0	2	9	0
2. Synaptic currents, qGluR	21	19	13	0.017–0.19	0.019–0.37	1.98–5.17	2.92–5.67	3.75 ± 0.43	3.84 ± 0.51	1	17	1	1	11	1
3. Patch Clamp, slow application, qGluR	11	11	5	0.022–0.18	0.011–0.30	3.27–4.72	3.18–4.38	3.99 ± 0.48	3.82 ± 0.42	0	11	0	0	5	0
4. Patch Clamp, fast application, qGluR	16	16	2	0.023–0.27	0.022–0.39	1.89–3.39	2.59–3.82	2.57 ± 0.5	3.21 ± 0.61	2	10	4	0	1	1

Four types of experiments were performed. The values of n were calculated from synaptic currents (for N-AChR and qGluR) and from the currents resulting from slow and fast agonist application (for qGluR). Each experiment was repeated several times (*Total*). The results for all types of experiment are given separately for second- and third-order polynomials. The number of successfully fitted polynomials was less than the total number of the experiments because the results of the remaining experiments did not meet the requirement set in Eq. 18.

model shown in Scheme 2. This simulation captured the findings of Colquhoun and Sakmann.

$$\begin{array}{ccccc} R_o + A & \overset{k_1}{\underset{k_{-1}}{\longleftrightarrow}} & R_1 & + A \overset{k_2}{\underset{k_{-2}}{\longleftrightarrow}} & R_2 \\ & & \underset{k_{o1}}{\updownarrow}\ k_{c1} & & \underset{k_{o2}}{\updownarrow}\ k_{c2} \\ & & O_1 & + A \overset{k_3}{\underset{k_{-3}}{\longleftrightarrow}} & O_2 \end{array}$$

SCHEME 2

Colquhoun and Sakmann (1985) fixed the values of the various rate constants to fit a membrane potential of −130 mV, whereas the rate constants that we used (Table 1) were established for resting potential. For Scheme 2, therefore, we also used the rate constants of Table 1 and supplemented them with the values of k_{o1}, k_{c1}, k_3, and k_{-3}. The values of k_{o1} and k_{c1} were chosen to conserve the relationships with k_{o2} and k_{c2}, respectively, as given by Colquhoun and Sakmann (1985). We simulated the model shown in Scheme 2 with a linearly increasing agonist concentration and transformed the obtained P_o into the reciprocal function $t(P_o/P'_o)$ (Fig. 7 *A*, *empty squares*). The third-order polynomial (*solid line*) was successfully fitted. The obtained value of $b_1 = 4.28$ suggests two binding sites (Eqs. 12 and 17). This result can be explained by the fact that k_{o1} is four orders of magnitude smaller than k_{o2}, and, therefore, the channel's probability of being in state O_1 is much smaller than its probability of being in state O_2. To determine conditions for which the presented method will yield $n = 1$, we increased the ratio k_{o1}/k_{o2} to 2 and analyzed the results of the simulations. Figure 7 *B* shows the simulation results for this case. As shown, only when the ratio $k_{o1}/k_{o2} \geq 1$ (four orders of magnitude higher than in the real case described by

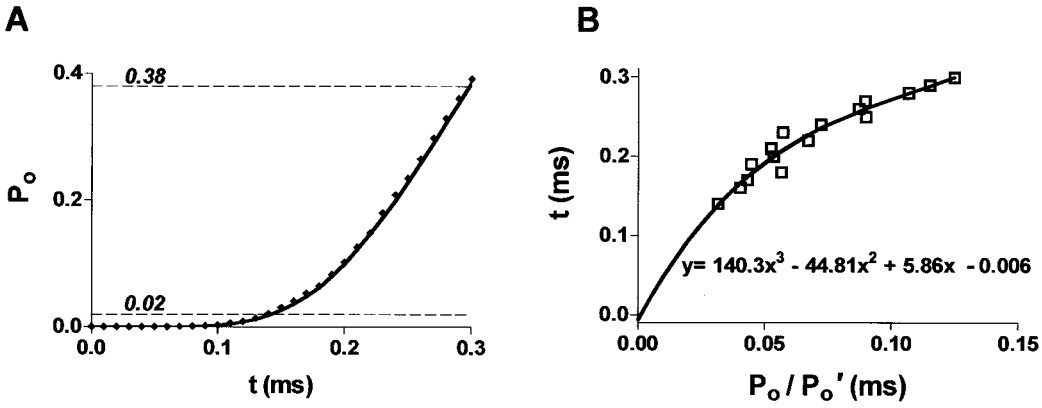

FIGURE 6 Example of the polynomial fit of the simulation results obtained using Monte-Carlo method with linearly increasing agonist concentration. Standard slow set of parameters was used for simulations (Table 1). (*A*) The initial phase of the simulated current. Average current from 10,000 single channels is shown as filled squares, and the current that obtained for the same model using the numerical solution of the differential equation is shown as a solid line. The region between the dashed lines is then transformed to the function $t(P_o/P'_o)$. (*B*) Third-order polynomial fit of $t(P_o/P'_o)$. *Empty squares*, the values of the function; *solid line*, polynomial fit. The obtained value of b_1, 5.86, suggests the correct number $n = 3$ (Eq. 17).

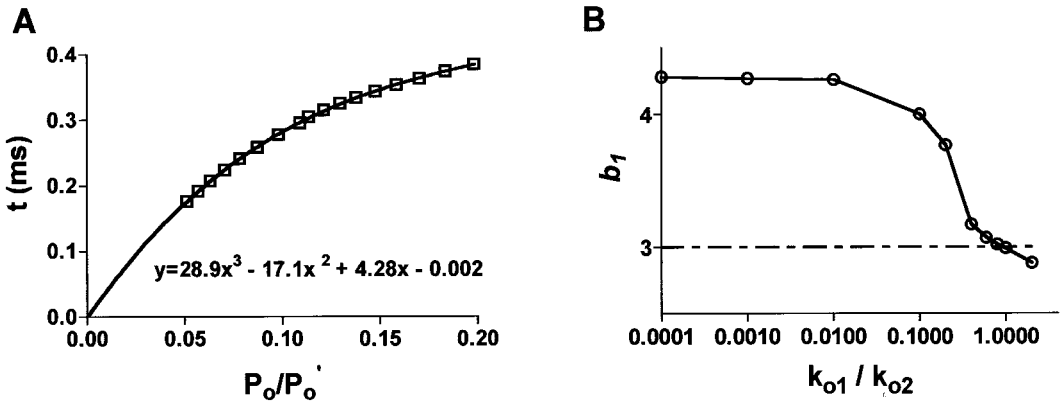

FIGURE 7 Analysis of opening from the partially liganded state. The open probability, P_o, in this case, is equal to $P_{o1} + P_{o2}$, where P_{o1} and P_{o2} are the channel's probabilities of being in states O_1 and O_2, respectively. (*A*) Calculation of n for the model shown on Scheme 2. The value of k_3 was assigned to be equal to k_2, and the value of k_{-3} was chosen to conserve energy. $k_{o1} = 0.0001 \cdot k_{o2}$, $k_{c1} = 10 \cdot k_{c2}$ (Colquhoun and Sakmann, 1985; see Table 1 for the values of the other rate constants). The obtained value of $b_1 = 4.28$ suggests two binding sites (Eq. 17). (*B*) The obtained value of b_1 (*empty circles*) as a function of the ratio k_{o1}/k_{o2}. When this ratio is less than 1, the obtained value of b_1 is greater, than 3 (*dashed line*), and, therefore, suggests that $n = 2$. When this ratio is greater than or equal to 1, the obtained value is less than 3, and suggests $n = 1$ (Eq. 17).

Colquhoun and Sakmann, 1985) does the obtained value of b_1 suggest $n = 1$. Below this ratio, in spite of an opening from a single-bound receptor, the evaluated n will be two.

DISCUSSION

In the present study, we propose a theoretical–experimental approach for calculating the number of agonist molecules, n, that must be bound for a receptor channel to open. This method is based on analysis of the initial phase of the MEPSC or current produced by agonist application to outside-out patches. Unlike the methods used in previous studies (see references in Introduction), our method is based on analysis of an analytical function $t(P_o/P'_o)$ rather than on numerical reconstruction of the current or dwell-time histograms. The advantage of this method is that it requires neither an initial model nor knowledge of the rate constant values.

Let us examine factors that may affect the accuracy of this method. The factors to be considered relate to experimental conditions and the recording system. To maximize precision in measuring the initial phase of the current, the signal-to-noise ratio must be increased as much as possible. To achieve this, a high concentration of agonist must be used. Indeed, in our experiments, a saturate concentration of glutamate, 10 mM (Tour et al., 1995) was used. An additional way to increase the signal-to-noise ratio is to record and average a sufficiently large number of currents. Conducting the experiments at low temperature also reduces the total noise by reducing the white noise. Low temperature also decreases the reaction rates, thereby causing a slower rise time. This permits sampling more data points during the initial rising phase of the current. For all the above reasons, the experiments presented here were conducted at low temperature.

Another important factor concerns filtration of the data. High filtration causes smoothing of the current, and consequently, reduces P'_o, increasing the value of P_o/P'_o. Ideally, the currents should be recorded with no filtration at all, but practically, this is impossible, given that the recording system has built-in filtration (approximately 100 kHz; Ogden, 1994). For the same reason, the frequency of the analog-to-digital conversion of the recorded currents must be as high as possible. We recorded the data of our experiments without additional filtration and sampled the data at 0.01 ms per point.

For the case of constant agonist concentration, the time required to increase agonist concentration from zero to its assigned value must be as short as possible. We managed to reduce this time to 0.16 ms. Precise definition of the longest permissible time is beyond the scope of the present study. However, preliminary analysis using computer simulations shows this value to be less than 0.11 ms (analysis not shown). It follows that the time interval during which the data may be collected for evaluation of the initial rise must be expanded. However, enlarging the interval of the approximation above the permissible value, P_v, causes the obtained value of n to decrease (see Theoretical Methods). As a result of the various sources of inaccuracy, n cannot be determined based on constant agonist concentration experiments alone. Conclusions regarding the true value of n, 2, were also confirmed by results of experiments in which agonist concentration rises linearly (Fig. 5, *B* and *C*). This result is in accord with the value of n estimated for the same preparation from measurements of the Hill coefficient (Tour et al., 1999). Our value of 2 differs, however, from results obtained by Dudel et al., 1990a,b for the same preparation.

The obtained value also agrees with estimates obtained in other systems: for AMPA subtype glutamate receptors in pyramidal cells of the rat hippocampus (Johans and Sak-

mann, 1992), for glutamate-activated channels in the visual cortex (Hestrin, 1992), and for AMPA receptors from cultured hippocampal neurons (Clements et al., 1998). The first two estimates were obtained using measurements of the Hill coefficient. Clements et al. (1998) estimated the value of n from the best fit of these models to the initial phase of the current at low concentration of agonist. Clements et al. confirmed their estimations by analysis of the antagonist displacement experiments.

Rosenmund et al. (1998), also using antagonist displacement experiments, suggested that a conformational change (achieved by binding agonist) in two subunits of the tetrameric receptor is sufficient to open the channel to a certain extent. Conformational changes in additional subunits open the pore further. We believe that our theory accounts for this case also, and the actual value of the observed n will yield the minimal number of agonist molecules needed to open the channel (see Fig. 7).

The Hill plot is by far the most common method used to evaluate n. The method used here offers several advantages over the Hill plot. First and most important, it does not require lengthy and complex experiments such as establishing a dose–response curve. Rather, it uses MEPSCs, which are obtained as a result of conducting routine experiments associated, for example, with release of neurotransmitter. Second, it does not require measurements at low agonist concentrations, measurements that are experimentally difficult to perform and result in noisy data. Third, the "run down" phenomenon, (Hestrin, 1992; Johans and Sakmann, 1992; Tour et al., 1995), which greatly affects the Hill plot, has no effect whatsoever on the precision of our method. Finally, because, in the proposed method we analyze only the initial phase of the current, desensitization, which affects the Hill plot, does not affect the analysis presented here.

The main disadvantage of our method is that its precision depends on the time resolution of the recording system; hence very fast processes, caused, for example, by positive cooperativity, can be overlooked. However, the precision of this method can be increased in the future. Several investigators have recently reported application systems with a stabilization time shorter than 0.1 ms (Maconochie et al., 1994; Heckmann et al., 1996).

We developed our method assuming a single opening from the fully liganded receptor—a widely accepted property of ligand-gated receptors. Existence of an additional opening from the partially liganded receptor, suggested, for example, by Colquhoun and Sakmann (1985) for the nicotinic receptor, can also affect the accuracy of the proposed method. We show that, for the nicotinic receptor, to see the minimal number of sites that must be bound for the receptor to open, the opening rate from the partially liganded state should be the same as the opening rate from the fully liganded state, (that is, the number of bindings that causes the opening from the partially liganded state). This disadvantage is shared by the Hill plot method.

To conclude, this new method can be a powerful instrument for determining the number of binding sites of ligand-gated receptor channels. In addition, the proposed method can be used to calculate the number of steps preceding the opening of voltage-dependent channels. Because the membrane potential can be changed experimentally in several microseconds, the equations for the case of constant agonist concentration are suitable. It appears that the analytical method presented can be a promising addition to the existing methods in this field (e.g., Hodgkin and Huxley, 1952; Mika and Palti, 1994).

APPENDIX A. THE EXPRESSION OF THE FIRST DERIVATIVE OF FUNCTION (P_o/P'_o) (t)

Constant agonist concentration

The following system of differential equations describes the kinetic model of Scheme 1.

$$\begin{aligned}
P'_{\mathrm{o}} &= -k_{\mathrm{c}} \cdot P_{\mathrm{o}} + k_{\mathrm{o}} \cdot R_{\mathrm{n}} \\
R'_{\mathrm{n}} &= k_{\mathrm{c}} \cdot P_{\mathrm{o}} - (k_{\mathrm{o}} + k_{-(\mathrm{n})}) \cdot R_{\mathrm{n}} + k_{(\mathrm{n})} \cdot A \cdot R_{\mathrm{n}-1} \\
&\vdots \\
R'_{\mathrm{i}} &= k_{-(\mathrm{i}+1)} \cdot R_{\mathrm{i}+1} \\
&\vdots \quad - (k_{-(\mathrm{i})} + k_{(\mathrm{i}+1)} \cdot A) \cdot R_{\mathrm{i}} + k_{(\mathrm{i})} \cdot A \cdot R_{\mathrm{i}-1} \\
R'_1 &= k_{-2} \cdot R_2 - (k_{-1} + \mathrm{k_2 \cdot A}) \cdot \mathrm{R_i} + k_1 \cdot A \cdot R_0 \\
R'_0 &= k_{-1} \cdot R_1 - k_1 \cdot A \cdot R_0.
\end{aligned} \tag{A1}$$

With the initial conditions,

$$\begin{aligned}
&P_{\mathrm{o}}(0) = 0, \\
&R_{\mathrm{i}}(0) = \begin{cases} 1 & \text{if} \quad i = 0 \\ 0 & \text{if} \quad i > 0. \end{cases}
\end{aligned} \tag{A2}$$

The general solution of Eqs. A1 and A2 is,

$$P_{\mathrm{o}}(t) = \sum_{\mathrm{i}=0}^{\mathrm{n}} C_{\mathrm{i}} \cdot e^{-\lambda_{\mathrm{i}} \cdot \mathrm{t}}, \tag{A3}$$

where C_{i} represents the weight of the ith exponent, and λ_{i} stands for its decay constant. Notice that $\lambda_0 = 0$ and λ_{i} is always positive.

We now show that $(P_o/P'_o)'_{t=0} = 1/(n+1)$. Because the solution of Eqs. A1 and A2 is a smooth function (Eq. A3), both $P_{\mathrm{o}}(t)$ and $P'_{\mathrm{o}}(t)$ can undergo Taylor expansion at the vicinity of $t = 0$. Formally,

$$\frac{P_{\mathrm{o}}}{P'_{\mathrm{o}}}(t) = \frac{P_{\mathrm{o}}(0) + \sum_{\mathrm{j}=1}^{\infty} [P_{\mathrm{o}}^{(\mathrm{j})}(0)/j!] \cdot t^{\mathrm{j}}}{P'_{\mathrm{o}}(0) + \sum_{\mathrm{j}=1}^{\infty} [P_{\mathrm{o}}^{(\mathrm{j}+1)}(0)/j!] \cdot t^{\mathrm{j}}}. \tag{A4}$$

The indices in the brackets above P_{o} denote the order of the time derivative, excepting the first derivative that is marked as P'_{o}.

Using sequential incorporation of the initial conditions (Eq. A2) into the system of differential equations (Eq. A1) we can show that, for $j = n + 1$,

$$P_o^{(j)} = \sum_{i=0}^{j-1} (-1)^{j-i} \cdot a_i \cdot P_o^{(i)} + \sum_{i=0}^{j-1} (-1)^{j-i-1} u_{n-i} \cdot R_{n-i}, \quad \text{(A5)}$$

where a_i and u_i are positive constants that depend only on rate constants and A. Using the mathematical induction method, we proved that

$$P_o^{(j)}(0) = \begin{cases} 0 & \text{if } j < n+1 \\ u_0 > 0 & \text{if } j = n+1. \end{cases} \quad \text{(A6)}$$

Incorporating Eq. A6 into Eq. A4 and rearranging gives

$$\frac{P_o}{P_o'}(t) = \frac{t}{n+1} \cdot \frac{P_o^{(n+1)}(0) + \frac{P_o^{(n+2)}(0)}{n+2} \cdot t + \frac{P_o^{(n+3)}(0)}{(n+2)(n+3)} \cdot t^2 + \cdots}{P_o^{(n+1)}(0) + \frac{P_o^{(n+2)}(0)}{n+1} \cdot t + \frac{P_o^{(n+3)}(0)}{(n+1)(n+2)} \cdot t^2 + \cdots}. \quad \text{(A7)}$$

Deriving Eq. A7, with respect to t, at $t = 0$, gives

$$\left(\frac{P_o}{P_o'}\right)'_{t=0} = \frac{1}{n+1}. \quad \text{(A8)}$$

Linearly increasing agonist concentration

To adapt the model to a linearly increasing agonist concentration, we supplement Eqs. A1 and A2 with

$$A = \alpha \cdot t. \quad \text{(A9)}$$

The solution of Eqs. A1, A2, and A9 is,

$$P_o(t) = \sum_{i=0}^{n} W_i \cdot e^{\lambda_i t}. \quad \text{(A10)}$$

Although C_i in Eq. A3, (constant agonist concentration) is constant, W_i in Eq. A10 is a polynomial function of t.

To derive the final expression for linearly rising agonist concentration, we use the same steps used to derive the final expression for constant agonist concentration (Eqs. A4–A8). We therefore mention only the key steps.

We begin with a Taylor expansion of the expression $(P_o/P_o')(t)$ and find it to equal Eq. A4. Using sequential incorporation of the initial conditions (Eq. A2) into the system of differential equations (Eq. A1 and A9) we can show that, for $j = 2n + 1$,

$$P_o^{(j)} = \sum_{i=0}^{j-1} (-1)^{j-1} \cdot a_i \cdot P_o^{(i)} + \sum_{i=0}^{(\text{int})(j/2)-1} d_i \cdot R_{n-i} + t \cdot \sum_{i=0}^{j-1} (-1)^{j-i-1} u_{n-i} \cdot R_{n-i}, \quad \text{(A11)}$$

where a_i, d_i, and u_i are positive constants, which depend only on rate constants and α. Using the mathematical induction method, we proved that

$$\lim_{t \to 0} P_o^{(j)} = \begin{cases} 0 & \text{if } j < 2n+1 \\ u_0 > 0 & \text{if } j = 2n+1. \end{cases} \quad \text{(A12)}$$

Equation A12, in this case, is analogous to Eq. A6. Incorporating Eq. A12 into Eq. A4 gives (similar to Eq. A6)

$$\frac{P_o}{P_o'}(t) = \frac{t}{2n+1} \cdot \frac{P_o^{(2n+1)}(0) + \frac{P_o^{(2n+2)}(0)}{2n+2} \cdot t + \frac{P_o^{(2n+3)}(0)}{(2n+2)(2n+3)} \cdot t^2 + \cdots}{P_o^{(2n+1)}(0) + \frac{P_o^{(2n+2)}(0)}{2n+1} \cdot t + \frac{P_o^{(2n+3)}(0)}{(2n+1)(2n+2)} \cdot t^2 + \cdots}. \quad \text{(A13)}$$

By deriving Eq. A13, with respect to t, at $t = 0$, we obtain (similar to Eq. A8)

$$\left(\frac{P_o}{P_o'}\right)'_{t=0} = \frac{1}{2n+1}. \quad \text{(A14)}$$

APPENDIX B. EXISTENCE AND PROPERTIES OF THE FUNCTION $(P_o/P_o')(t)$

The function $f(t)$ has a smooth, monotonous reciprocal function, $t(f)$, if $f(t)$ is smooth and monotonous and the first derivative of the function $f(t)$ at $t = 0$ exists (Courant, 1965). In principle, it is possible to prove by mathematical analysis that the function $(P_o/P_o')(t)$ is smooth and monotonous. A complex proof of this sort, however, is beyond the scope of the present study. We therefore choose to illustrate that, for a wide range of parameters, the function $(P_o/P_o')(t)$ does demonstrate such behavior. Figure *B*1 shows simulation results of a model with $n = 3$ and a set of parameters for low temperature at (*A*) constant and (*B*) linearly increasing concentrations. Each graph shows the behavior of $(P_o/P_o')(t)$ with the increase and decrease of one of the model rate constants, whereas all other constants retain their default values. As can be seen, in all these cases, the function $(P_o/P_o')(t)$ behaves as a smoothly and monotonically increasing function. Because the first derivative of the function $(P_o/P_o')(t)$ at $t = 0$ exists (Eqs. 5 and 6), we can safely conclude that, for a very wide range of parameters, the reciprocal function, $t(P_o/P_o')$ exists and it is smooth and monotonous.

APPENDIX C. EXPRESSIONS FOR b_2 (FROM EQS. 14 AND 15) AND b_3 (FROM EQ. 15)

We begin with the case of constant agonist concentration. Taylor coefficients b_1 and b_2 are given by the corresponding derivatives of the reciprocal function, as follows:

$$b_2 = \frac{1}{2} \cdot t^{(2)} \left(\frac{P_o}{P_o'}\right)\Big|_0, \quad \text{(C1)}$$

$$b_3 = \frac{1}{6} \cdot t^{(3)} \left(\frac{P_o}{P_o'}\right)\Big|_0. \quad \text{(C2)}$$

Calculating the derivatives in Eqs. C1 and C2, we obtain

$$b_2 = -\frac{1}{2} \cdot \frac{(P_o/P_o')^{(2)}(0)}{((P_o/P_o')'(0))^3}, \quad \text{(C3)}$$

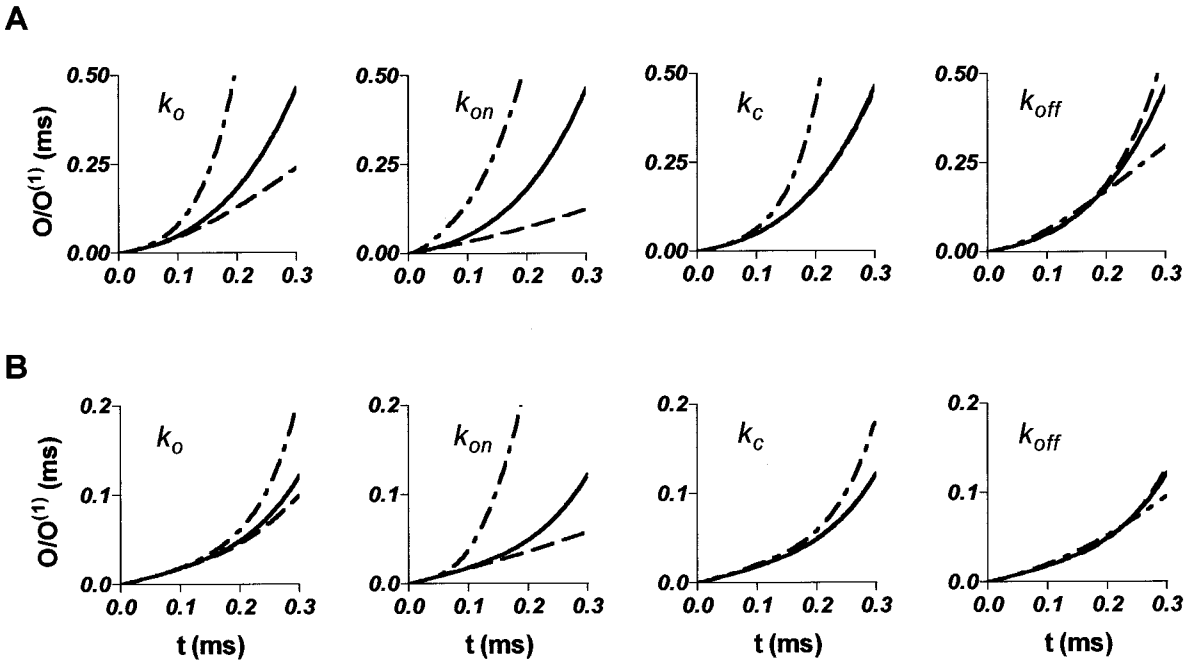

FIGURE B1 Illustration that the function $(P_o/P'_o)(t)$ is smooth and monotonous for a very wide range of parameters—simulation results. Each rate constant [open rate (k_o), close rate (k_c), on (k_1, k_2, and k_3), and off rates (k_{-1}, k_{-2}, and k_{-3})] was increased (*striped line*) and decreased (*dashed line*) ten times compared to a default set of parameters (*solid line*). (*A*) Constant agonist concentration. (*B*) Linearly increased agonist concentration.

$$b_3 = \frac{1}{6}\cdot\frac{\left(\frac{P_o}{P'_o}\right)^{(3)}(0)\cdot\left(\frac{P_o}{P'_o}\right)'(0) - 3\cdot\left(\left(\frac{P_o}{P'_o}\right)^{(2)}(0)\right)^2}{\left(\left(\frac{P_o}{P'_o}\right)'(0)\right)^5}. \tag{C4}$$

Deriving Eq. A7, we obtain

$$\left(\frac{P_o}{P'_o}\right)'(0) = \frac{1}{n+1}, \tag{C5}$$

$$\left(\frac{P_o}{P'_o}\right)^{(2)}(0) = 2\cdot\frac{-P_o^{(n+2)}(0)}{(n+1)^2\cdot(n+2)\cdot P_o^{(n+1)}(0)}, \tag{C6}$$

$$\left(\frac{P_o}{P'_o}\right)^{(3)}(0) = -6\cdot\left(\frac{2\cdot P_o^{(n+3)}(0)}{(n+1)^2\cdot(n+2)\cdot(n+3)\cdot P_o^{(n+1)}(0)} + \frac{(P_o^{(n+2)}(0))^2}{(n+1)^3\cdot(n+2)\cdot(P_o^{n+1}(0))^2}\right). \tag{C7}$$

Incorporating Eqs. C5, C6, and C7 into Eqs. C3 and C4, we obtain

$$b_2 = \frac{n+1}{n+2}\cdot\frac{P_o^{(n+2)}(0)}{P_o^{(n+1)}(0)}, \tag{C8}$$

$$b_3 = \frac{2\cdot(n+1)^2\cdot P_o^{(n+3)}(0)}{(n+2)\cdot(n+3)\cdot P_o^{(n+1)}(0)} - \frac{n\cdot(n+1)\cdot(P_o^{(n+2)}(0))^2}{(n+2)^2\cdot(P_o^{(n+1)}(0))^2}. \tag{C9}$$

At this point, we must estimate the values of $P_o^{(n+2)}(0)$ and $P_o^{(n+3)}(0)$. First, we express these derivatives in terms of u_{n-i} and a_i (see Eq. A5). Then we express the necessary u_{n-i} and a_i through the corresponding rate constants.

Deriving Eq. A5, we obtain

$$P_o^{(n+2)} = \sum_{i=0}^{n}(-1)^{n-i+1}\cdot a_i\cdot P_o^{(i+1)} + \sum_{i=0}^{n}(-1)^{n-i}u_{n-i}\cdot R'_{n-i}. \tag{C10}$$

Separating the three last terms from the second sum in Eq. C10 gives

$$P_o^{(n+2)} = \sum_{i=0}^{n}(-1)^{n-i+1}\cdot a_i\cdot P_o^{(i+1)} + \sum_{i=0}^{n-3}(-1)^{n-i}u_{n-i}\cdot R'_{n-i} + u_2R'_2 - u_1R'_1 + u_0R'_0. \tag{C11}$$

Incorporating Eq. A1 into Eq. C11 and redefining the coefficients of R_i as q_i, we obtain

$$P_o^{(n+2)} = \sum_{i=0}^{n} (-1)^{n-i+1} a_i P_o^{(i+1)} + (-1)^n u_n k_c P_o + \sum_{i=0}^{n-2} (-1)^{n-i} q_{n-i} R_{n-1} + q_1 R_1 - q_0 R_0, \tag{C12}$$

where q_{n-i} is a linear combination of u_{n-i+1}, u_{n-i}, and u_{n-i-1}, such as,

$$q_0 = k_1 \cdot A \cdot (u_0 + u_1)$$
$$q_1 = k_2 \cdot A \cdot (u_2 + u_1) + k_{-1} \cdot (u_0 + u_1). \tag{C13}$$

Notice that q_0, q_1, and q_{n-i} are always positive. Incorporating Eqs. A6 and A2 into Eq. C12 gives

$$P_o^{(n+2)} = -(a_0 \cdot u_0 + q_0) < 0. \tag{C14}$$

Incorporating Eqs. C14 and A12 into Eq. C8 gives

$$b_2 = -\frac{n+1}{n+2} \cdot \frac{a_0 \cdot u_0 + q_0}{u_0} < 0. \tag{C15}$$

In a similar fashion, we calculate the value of $P_o^{(n+3)}$ for the purpose of estimating b_3. The final expression for b_3 is too complicated to be presented in this paper, but it can be shown that, independent of the values of the rate constants,

$$b_3 > 0. \tag{C16}$$

A more exact estimation for b_2 and b_3 is possible, but the process is beyond the scope of the present study.

Equations for b_2 and b_3 for the condition of linearly increasing agonist can be obtained by the same method used for constant agonist concentration.

We thank Gregory Rashkovan and Inna Fabricant for providing the experimental data shown in Figs. 3 and 5, *A* and *B*.

REFERENCES

Ashkenazi, G., and H. Parnas. 1997. Bioq homepage. http://www.ls.huji.ac.il/~parnas/Bioq/bioq.html.

Bates, S. E., M. S. P. Sansom, F. G. Ball, R. L. Ramsey, and P. N. R. Usherwood. 1990. Glutamate receptor-channel gating. Maximal likelihood analysis of gigaohm seal recordings from locust muscle. *Biophys. J.* 58:219–229.

Bloch, Z. L., I. M. Glagoleva, E. A. Lieberman, and V. A. Nenashev. 1968. A study of quantal transmitter release at a chemical synapse. *J. Physiol.* 199:11–35.

Buchman, E., and H. Parnas. 1992. Sequential approach to describe the time course of synaptic channel opening under constant transmitter concentration. *J. Theor. Biol.* 158:517–534.

Buchman, E., and H. Parnas. 1994. Sequential approach to describing channel opening and desensitization. *J. Theor. Biol.* 167:381–395.

Clements, J. D. 1996. Transmitter timecourse in the synaptic cleft: its role in central synaptic function. *Trends Neurosci.* 19:163–171.

Clements, J. D., A. Feltz, Y. Sahara, and G. L. Westbrook. 1998. Activation kinetics of AMPA receptor channels reveals the number of functional agonist binding sites. *J. Neurosci.* 18:119–127.

Clements, J. D., and G. L. Westbrook. 1991. Activation kinetics reveals the number of glutamate and glycine binding sites on the *N*-methyl-D-aspartate receptor. *Neuron.* 7:605–613.

Collingridge, G. L., and R. A. J. Lester. 1989. Excitatory amino acid receptors in the vertebrate central nervous system. *Pharmacol. Rev.* 41:143–210.

Colquhoun, D., and A. G. Hawkes. 1995. The principle of stochastic interpretation of ion-channel mechanism. *In* Single Channel Recording, 2nd ed. B. Sakmann and E. Neher, editors. Plenum Press, New York. 397–482.

Colquhoun, D., and D. C. Ogden. 1988. Activation of ion channels in the frog end-plate by high concentration of acetylcholine. *J. Physiol. (Lond.).* 395:131–159.

Colquhoun, D., and B. Sakmann. 1985. Fast events in single-channel currents activated by acetylcholine and its analogues at the frog muscle end-plate. *J. Physiol. (Lond.).* 369:501–557.

Courant, R. 1937a. Differential and Integral Calculus. 2nd ed. Bladel and Son, Ltd., Glasgo, UK. 144–153.

Courant, R. 1937b. Differential and Integral Calculus. 2nd ed. Bladel and Son, Ltd., Glasgo, UK. 315–341.

del Castillo, J., and Katz, B. 1957. Interaction at end-plate receptors between different choline derivatives. *Proc. R. Soc. Lond. [Biol].* 146: 369–381.

Dudel, J. 1983. Graded or all-or-nothing release of transmitter quanta by local depolarization of nerve terminals on crayfish muscle? *Pfluegers Arch.* 398:155–164.

Dudel, J. 1989. Calcium dependence of quantal release triggered by graded depolarization pulses to nerve terminals on crayfish and frog muscle. *Pfluegers Arch.* 415:289–298.

Dudel, J., C. Franke, and H. Hatt. 1990a. A family of glutamatergic, excitatory channel types at crayfish neuromuscular junction. *J. Comp. Physiol. A.* 166:757–768.

Dudel, J., C. Franke, and H. Hatt. 1990b. Rapid activation, desensitization, and resensitization of synaptic channels of crayfish muscle after glutamate pulses. *Biophys. J.* 57:300–306.

Dudel, J., and S. W. Kuffler. 1961. Presynaptic inhibition at the crayfish neuromuscular junction. *J. Physiol.* 155:543–562.

Dudel, J., M. Shramm, E. Ratner, and H. Parnas. 1999. Block of quantal end-plate currents of mouse muscle by physostigmine and procaine. *J. Neurophysiol.* 81:2386–2397.

Franke, C., H. Hatt, and J. Dudel. 1987. Liquid filament switch for ultra-fast exchanges of solutions at excised patches of synaptic membrane of crayfish muscle. *Neurosci. Lett.* 77:199–204.

Franke, C., H. Hatt, H. Parnas, and J. Dudel. 1991. Kinetic constants of the acetylcholine (ACh) receptor reaction deduced from the rise in open probability after step in ACh concentration. *Biophys. J.* 60:1008–1016.

Heckmann, M., J. Bufler, C. Franke, and J. Dudel. 1996. Kinetics of homomeric GluR6 Glutamate receptor-channels. *Biophys. J.* 71: 1743–1750.

Hestrin, S. 1992. Activation and desensitization of glutamate-activated channels mediating fast excitatory synaptic currents in the visual cortex. *Neuron.* 9:991–999.

Hodgkin, A. L., and A. F. Huxley. 1952. A quantitative description of membrane current 41 and its application to conditioning and excitation in nerve. *J. Physiol.* 117:500–544.

Hucho, F., V. I. Tselin, and J. Machold. 1996. The emerging three-dimensional structure of a receptor. The nicotinic acetylcholine receptor. *Eur. J. Biochem.* 239:539–557.

Johans, P., and B. Sakmann. 1992. Properties of AMPA subtype glutamate receptors in pyramidal cells of rat hippocampus. *J. Physiol. (Lond.).* 455:143–171.

Land, B. R., W. V. Harris, E. E. Salpeter, and M. M. Salpeter. 1984. Diffusion and binding constants for acetylcholine derived from the failing phase of miniature endplate currents. *Proc. Natl. Acad. Sci. USA.* 81:1954–1958.

Maconochie, D. J., and D. E. Knight. 1989. A method for making solution changes in the sub-millisecond range at the tip of a patch pipette. *Pflugers Arch.* 414:589–596.

Maconochie, D. J., J. M. Zempel, and J. H. Steinbach. 1994. How quickly can $GABA_A$ receptor open? *Neuron.* 12:61–71.

Magleby, K. L., and D. S. Weiss. 1990. Identifying kinetic gating mechanisms for ion channels using two-dimension distribution of simulated dwell times. *Proc. R. Soc. Lond. B.* 241:220–228.

McManus, O. B., D. S. Weiss, C. E. Spivak, A. L. Blatz, and K. L. Magleby. 1988. Fractal models are inadequate for the kinetics of four different ion channels. *Biophys. J.* 54:859–870.

Mika, Y. H., and Y. Palti. 1994. Charge displacement in a single potassium ion channel macromolecule during gating. *Biophys. J.* 67:1455–1463.

Ogden, D. 1994. Microelectrode electronics. *In:* Microelectrode Techniques. The Plymouth Workshop Handbook. David Ogden, editor. Cambridge, UK. 407–439.

Ogden, D., and P. Stanfield. 1994. Patch clamp techniques for single channel and whole cell recording. *In:* Microelectrode Techniques. The Plymouth Workshop Handbook. David Ogden, editor. Cambridge, UK. 53–79.

Parnas, H., M. Flashner, and M. E. Spira. 1989. Sequential model to describe the nicotinic synaptic current. *Biophys. J.* 55:875–884.

Parnas, I., and H. L. Atwood. 1966. Phasic and tonic neuromuscular systems in the abdominal extensor muscles of the crayfish and rock lobster. *Comp. Biochem. Physiol.* 18:701–723.

Prinz, H., and A. Maelicke. 1983. Interaction of cholinergic ligands with the purified acetylcholine receptor protein. I. Equilibrium binding studies. *J. Biol. Chem.* 258:10263–10271.

Rang, H. P. 1974. Acetylcholine receptors. *Q. Rev. Biophys.* 7:283–399.

Rosenmund, C., Y. Stern-Bach, and C. F. Stevens. 1998. The tetrameric structure of a glutamate receptor channel. *Science.* 280:1596–1599.

Stryer, L. 1981. Biochemistry. Chap. 4. Freeman & Co., San Francisco, CA.

Tour, O., H. Parnas, and I. Parnas. 1995. The double-ticker: an improved fast drug application system reveals desensitization of the glutamate channel from a closed state. *Eur. J. Neurosci.* 7:2093–2100.

Unwin, N. 1993. Nicotinic acetylcholine receptor at 9 Å resolution. *J. Mol. Biol.* 229:1101–1124.